Individual Single-Walled Carbon Nanotubes as Nanoelectrodes for Electrochemistry

ARTICLE *in* NANO LETTERS · FEBRUARY 2005

Impact Factor: 13.59 · DOI: 10.1021/nl048200m · Source: PubMed

NANO LETTERS

2005
Vol. 5, No. 1
137−142

Individual Single-Walled Carbon Nanotubes as Nanoelectrodes for Electrochemistry

Iddo Heller, Jing Kong,[†] Hendrik A. Heering, Keith A. Williams,[‡] Serge G. Lemay, and Cees Dekker*

Kavli Institute of Nanoscience, Delft University of Technology, Lorentzweg 1, 2628 CJ Delft, The Netherlands

Received October 31, 2004; Revised Manuscript Received November 26, 2004

ABSTRACT

We demonstrate the use of individual single-walled carbon nanotubes (SWNTs) as nanoelectrodes for electrochemistry. SWNTs were contacted by nanolithography, and cyclic voltammetry was performed in aqueous solutions. Interestingly, metallic and semiconducting SWNTs yielded similar steady-state voltammetric curves. We clarify this behavior through a model that considers the electronic structure of the SWNTs. Interfacial electron transfer to the SWNTs is observed to be very fast but can nonetheless be resolved due to the nanometer critical dimension of SWNTs. These studies demonstrate the potential of using a SWNT as a model carbon nanoelectrode for electrochemistry.

Electrodes with nanometer dimensions provide exciting new tools for electrochemical studies. The small dimensions lead to a high current density at the electrode surface, allowing the study of fast heterogeneous electron transfer kinetics, molecular interactions, and mass transport in the nanometer regime. In addition, exploiting the small dimensions of nanoelectrodes may allow innovative biological applications by means of probing local cellular environments and ultimately measuring the activity of a single redox-enzyme coupled to a nanoelectrode. Several techniques have been developed for the fabrication of nanoscale electrodes for electrochemistry.[1−5] However, no nanoelectrode fabrication technique has yet been developed where the electrode geometry is known at the nanometer level, which poses a limitation to the interpretation of electrochemical data.[6]

Here we explore the use of individual single-walled carbon nanotubes (SWNTs) as electrodes for electrochemistry. The unique structural and electronic properties[7,8] of a SWNT render it an ideal candidate to function as a model carbon nanoelectrode for electrochemistry. SWNTs have a very well defined cylindrical geometry and are readily synthesized[9] with a diameter in the nanometer range. Moreover, advances on the functionalization of SWNTs[8,10,11] open the route toward electrochemical single-biomolecule studies using individual SWNT electrodes.[12]

Large ensembles of carbon nanotubes have been used as electrode material for electrochemical experiments, which allowed exploring their high chemical stability and good conductive properties.[8] Although electrochemistry with an individual 150 nm diameter multiwalled carbon nanotube (MWNT) has been reported,[13] the unique structural properties of an individual SWNT as an electrode with a nanometer critical dimension have to our knowledge not been explored thus far.

We report the first study of electrochemistry using individual SWNT electrodes. We observe a steady-state electrochemical current that is proportional to the exposed length of the SWNT. Interestingly, both metallic and semiconducting SWNTs yield similar behavior. We demonstrate that this can be understood from a model that incorporates the electronic structure of the electrode into the estimation of heterogeneous electron-transfer kinetics. The experimental curves can be described by classic Butler−Volmer kinetics and show that the SWNT sidewall allows for high electron-transfer rates.

Figure 1a shows the device schematic consisting of a SWNT on a substrate contacted by leads that are covered by an insulating layer. SWNTs are grown through chemical vapor deposition[9] on a substrate consisting of a degenerately doped silicon wafer with a 500 nm thermally grown oxide layer. The sample is coated with a 20 nm electron-beam evaporated SiO_x layer.[14] After consequent resist patterning by electron-beam lithography, the SiO_x layer is briefly etched in a highly diluted buffered HF solution to expose the SWNTs. We contact the SWNTs by 40 nm thick titanium

* Corresponding author. E-mail: dekker@mb.tn.tudelft.nl.
[†] Present address: Department of Electrical Engineering and Computer Science, Massachusetts Institute of Technology, 77 Massachusetts Avenue, Cambridge, MA 02139-4307.
[‡] Present address: Department of Physics, University of Virginia, 382 McCormick Road, Charlottesville, VA 22904-4714.

10.1021/nl048200m CCC: $30.25
Published on Web 12/17/2004

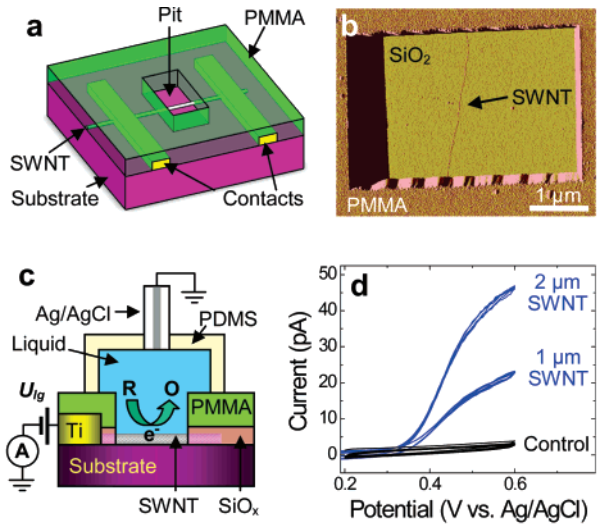

Figure 1. (a) Device schematic. SWNTs are grown on Si wafers with 500 nm thermal SiO_2 and contacted by Ti leads. A layer of SiO_x and PMMA is used as insulating layer, in which windows are opened to selectively expose the SWNTs. (b) AFM-amplitude image of an exposed section of a SWNT crossing the bottom of the pit through the PMMA and SiO_x layers. (c) Low current measurement setup. The SWNT is exposed to a solution containing a redox-active species. To avoid evaporation during measurements, the solution is contained by a PDMS cell. A potential is applied to the SWNT versus a standard Ag/AgCl 3M NaCl electrode. (d) Sampled current voltammograms measured from two metallic SWNT devices (1 μm and 2 μm exposed) and a control device exposed to an aqueous 1.2 mM $FcTMA^+$ solution. The control device consists of a pit located near the leads but without a SWNT. Three full forward and backward scans are plotted for each device. The good overlap shows that the voltammograms are well reproducible.

leads. A 500 nm poly(methyl methacrylate) (PMMA) layer is coated on the entire surface, which serves as an insulating layer to prevent electrochemical reactions taking place at the leads. In addition, the titanium has a natural oxide that further suppresses any leakage current. Micrometer-sized rectangular pits are patterned in the PMMA to partially expose the contacted SWNTs. The pits are created at a distance of at least several hundreds of nanometers away from the leads. Figure 1b shows an AFM amplitude image in which an exposed section of SWNT is visible crossing the bottom of the pit in the PMMA insulation. The titanium leads are not visible under the PMMA. Whether each individual SWNT is semiconducting or metallic is determined through electrical transport measurements in air using the silicon wafer as a backgate prior to electrochemical measurements.[15]

The devices were exposed to aqueous solutions containing reduced ferrocenylmethyl-trimethylammonium ($FcTMA^+$), with counterion hexafluorophosphate (PF_6^-).[5] $FcTMA^+$ was chosen for its uncomplicated electrochemistry and its good chemical stability in an aerobic aqueous environment. No supporting electrolyte was used. To minimize evaporation, the solution was contained by a poly(dimethylsiloxane) (PDMS) cell pressed against the sample and sealed using a commercial Ag/AgCl 3M NaCl reference electrode (model MF-2078, BAS). Sampled-current voltammetry was performed in a low-current measurement setup as depicted in Figure 1c using the SWNT as the working electrode. An electrometer (Keithley 6430) was used to cycle the potential applied to the SWNT between 0.2 and 0.6 V with respect to the grounded Ag/AgCl reference electrode. Typically, the current is sampled over 0.2 s after a delay of 0.1 s per 10 mV step.

We observed a steady-state electrochemical current through the SWNT devices. In Figure 1d, we show the cyclic voltammograms acquired from two metallic SWNT devices of different exposed length, and a control device on the same wafer. At high potential, an anodic current was observed that corresponds to the oxidation of $FcTMA^+$. The magnitude of the steady-state electrochemical current is of the order of several picoamperes and scales with the length of the exposed section of SWNT. The black curve in Figure 1d is a measurement for a control pit that lacks a SWNT on the same wafer. This control pit was created near titanium leads similar to the SWNT devices and displayed no electrochemical wave due to the absence of a SWNT. These measurements show that the electrochemical current can be attributed to the oxidation of $FcTMA^+$ at the SWNT sidewall, and the titanium leads are sufficiently insulated from solution.

The voltammetric curves obtained from the SWNT devices deviate from the classic nernstian curve-shape controlled by thermodynamics and mass transport. Within the scanned potential window we do not observe a diffusion-limited plateau and the voltammetric waves appear stretched. We attribute this to the heterogeneous electrode kinetics that control the rate of the electrode reaction. Due to the small critical dimension of the SWNT, mass transport is highly effective, and the rate of mass transport may become comparable to or larger than the rate of electron transfer. In this case there will be a deviation from thermodynamic equilibrium between oxidized and reduced species at the electrode surface and the voltammetric curve will depart from the nernstian limit.

In total we fabricated four wafers with multiple devices per wafer. The devices on one wafer are processed simultaneously. We measured 43 devices, of which 11 devices gave no or poor waves, which may be attributed to the breakdown or contamination of devices. The remaining 32 devices yielded a range of voltammetric behavior similar to the curves displayed in Figure 2a and 2b. Although the deviation from nernstian voltammetry varies between the curves, the shape is relatively consistent for simultaneously processed devices, suggesting that the observed variations are related to sample preparation. We tentatively attribute this to contamination of the SWNT surface, which can effectively slow the rate of electron transfer, changing the classic nernstian appearance of the steady-state current−potential characteristics.

We used both metallic and semiconducting SWNT devices for electrochemistry, as shown in Figure 2a and 2b, respectively. Interestingly, no significant difference in electrochemical properties was found. In Figure 2c we plot the electrochemical current at 0.6 V against the exposed length of SWNT for all devices of the wafer for which the voltammograms displayed the smallest departure from nerns-

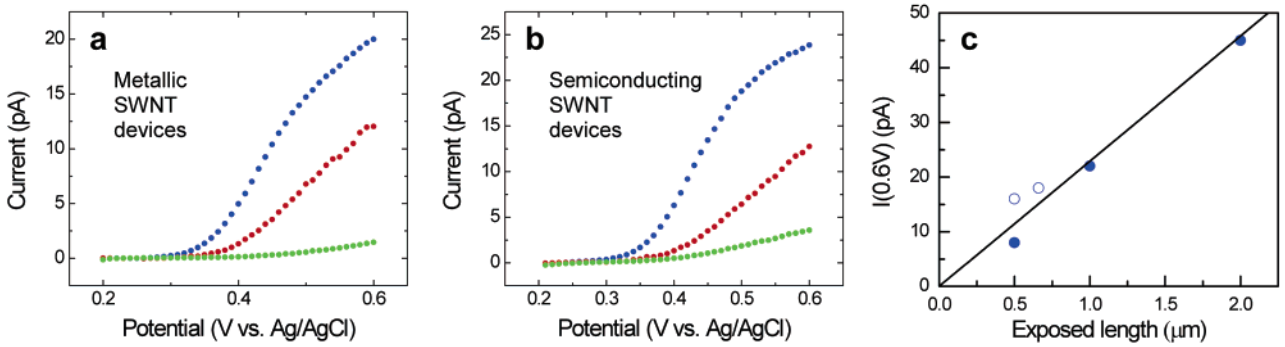

Figure 2. Sampled-current voltammograms (three averaged forward scans) of the oxidation of 1.2 mM $FcTMA^+$ at (a) three metallic and (b) three semiconducting SWNT devices. The blue curves are devices from one wafer and the red and green curves are the devices on another wafer. The data were collected in absence of supporting electrolyte. The exposed lengths of SWNT for the metallic devices were, from top to bottom 1, 2, and 0.6 μm, and for the semiconducting devices 0.75, 1.75, and 0.8 μm. (c) The electrochemical current at 0.6 V vs Ag/AgCl exhibits a linear dependence on the exposed length of SWNT within one wafer. The closed circles indicate devices where the SWNT crosses the entire bottom of the pit, and open circles indicate devices where the pit was created over the end of a SWNT and thus the SWNT does not span the entire bottom of the pit, resulting in more effective mass transport and a consequently higher current density.

tian voltammetry, i.e., the devices that are considered to be the least or not contaminated. A linear fit through the origin is shown yielding $I(0.6\ \text{V}) = 22 \pm 1$ pA/μm. Devices on other presumably more contaminated wafers display a smaller current per μm of exposed SWNT. The reduced current, combined with the departure from the nernstian voltammetric curve shape, is consistent with a kinetic limitation on the reaction rate.

The enhanced mass transport rate at a nanoelectrode allows the kinetics of electrode reactions to be accessed through voltammetry. Using the classic Butler−Volmer model of electrode kinetics, the oxidative current i_{BV} for a one-step, one-electron process can be written as[16]

$$i_{BV} = \frac{i_{mt}}{1 + e^{-F(U-U^{0'})/RT} + K_0^{-1} e^{-F(1-\alpha)(U-U^{0'})/RT}} \qquad (1)$$

Here i_{mt} is the mass-transport-limited current, F is the Faraday constant, R is the molar gas constant, T is absolute temperature, U is the applied potential, $U^{0'}$ is the formal potential of the redox-couple, α is the transfer coefficient, and K_0 is the dimensionless heterogeneous rate constant,[16] $K_0 = FACk^0/i_{mt}$, where A is the electrode surface area, C the bulk concentration of the reduced species, and k^0 the standard heterogeneous rate constant. Figure 3 shows a fit of eq 1 to the experimental data using k^0, α, and i_{mt} as fitting parameters. $U^{0'}$, A, and C are fixed, where $U^{0'} = 0.42$ V, $C = 1.2$ mM, and A was calculated as πrL, where the radius r of the SWNT was determined from AFM. Equation 1 appears to provide an excellent description of the experimental curve shape. The fit of Figure 3 yields $k^0 = 7.62 \pm 0.03$ cm/s, $\alpha = 0.670 \pm 0.002$ and $i_{mt} = 48.4 \pm 0.1$ pA.

We fitted eq 1 for all devices of Figure 2c yielding an average $\alpha = 0.65 \pm 0.07$ and $k^0 = 4 \pm 2$ cm/s. We performed a linear regression of the fitted mass-transport-limited currents versus the exposed lengths, yielding $i_{mt} = 24 \pm 2$ pA/μm. The high k^0 value, comparable to common metallic electrodes, indicates that the SWNT sidewall allows very fast electron transfer. Indeed, the values are in very

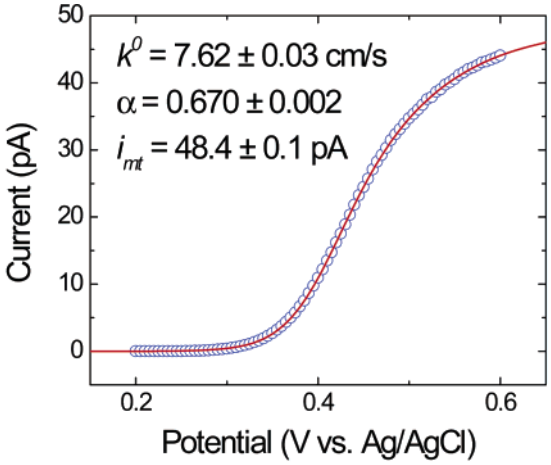

Figure 3. Fit of the classic Butler−Volmer kinetics of eq 1 to the experimental voltammogram of a 2 μm long metallic SWNT with a 1.8 nm diameter, using $U^{0'} = 0.42$ mV and $C = 1.2$ mM.

good agreement with values measured by Watkins and coworkers, who found $\alpha = 0.6 \pm 0.2$ and $k^0 = 5 \pm 3$ cm/s for the oxidation of $FcTMA^+$ at platinum nanoelectrodes.[6] Further research is needed to determine to what extent this high electron-transfer rate is intrinsic to the sidewall of the SWNT or should be attributed to surface defects along the SWNT sidewall.

Two further remarks can be made with respect to the curve fitting of Figure 3. First, no contamination of the SWNT surface was taken into account. As a result of a potential extra tunneling barrier and reduced electroactive area on the SWNT, the result for the heterogeneous rate constant may be underestimated. Second, the data were acquired in the absence of supporting electrolyte. Although caution should be taken to interpret voltammetric curves acquired in the absence of supporting electrolyte, preliminary measurements in the presence of a supporting electrolyte (0.1 M KCl) show the same current−potential curve shape, indicating that the electrical double-layer has little effect on voltammetry at the SWNT electrode. Indeed, due to the high aspect ratio, the depletion layer around the SWNT is about 2 orders of magnitude larger than the electrical double-layer, which is

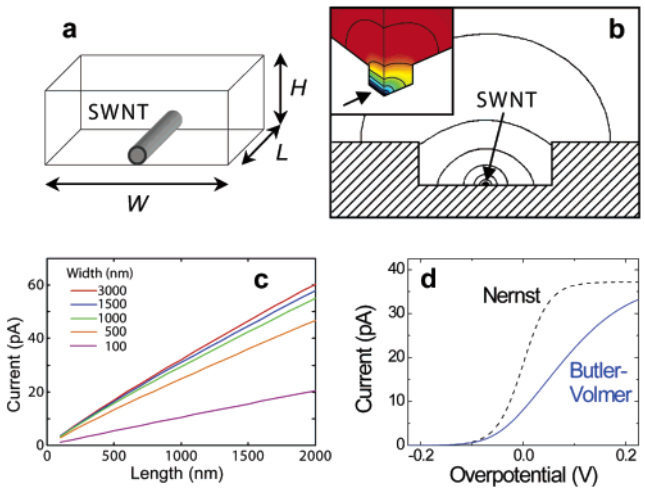

Figure 4. Numerical simulation of the diffusion-limited current and voltammetric behavior. (a) A SWNT crossing the bottom of the pit in the PMMA. (b) Cross section of the three-dimensional steady-state concentration profile perpendicular to the SWNT axis with contour lines calculated by a finite-element method. Inset: three-dimensional view of the calculated concentration profile cross-sectioned both perpendicular to the SWNT and through the SWNT axis. Blue and red indicate the reactant concentrations at the SWNT surface and the bulk respectively, the arrow indicates the position of the SWNT. (c) Calculated steady-state diffusion-limited current for a 1 nm radius SWNT as a function of the exposed length for different pit widths W. $H = 0.5$ μm. (d) Calculated electrochemical current as a function of overpotential ($U - U^{0'}$) for a SWNT electrode of 1 nm radius in a pit with dimensions $L = 1$ μm, $W = 1.5$ μm, and $H = 0.5$ μm, using $k^0 = 4$ cm/s and $\alpha = 0.65$ (solid blue line). The dashed line indicates the nernstian limit, $K^0 \rightarrow \infty$.

expected to minimize the influence of the electrical double-layer on molecular transport.

We estimated the steady-state diffusion-limited current using a finite element package (Femlab3.0a, COMSOL AB) to solve the three-dimensional diffusion equation for a SWNT device with the geometry as defined in Figure 4a. The resulting steady-state concentration profile in Figure 4b shows a gradual transition from cylindrical diffusion near the SWNT to spherical diffusion toward the bulk. Due to the spherical diffusion field, the SWNT device behaves like a common microelectrode, giving a steady-state current despite its cylindrical electrode shape.

We performed a series of simulations for a 1 nm radius SWNT in a pit of height (H) 0.5 μm, varying the width (W) and length (L), as displayed in Figure 4c. Indeed as was experimentally observed, the electrochemical current is proportional to the exposed length of the SWNT. In addition, the electrochemical current is rather independent of W, provided that $W > 2H$. The diffusion-limited current has a weak dependence on the radius of the SWNT. For example, doubling the radius of the SWNT typically causes a mere 10% increase of the diffusion-limited current. The calculations show that a device of a 1 nm radius SWNT crossing a pit with dimensions $L = 1$ μm, $W = 1.5$ μm, and $H = 0.5$ μm gives a diffusion-limited current of 37 pA for a bulk concentration of 1.2 mM $FcTMA^+$ using a diffusion coefficient $D = 7.5 \times 10^{-6}$ cm^2/s.[17] Note that the end of a SWNT, modeled as a 1 nm radius hemispherical electrode for which $i_{mt} = 2\pi FDCr$, would by itself give only a 0.5 pA diffusion-limited current, which shows that the experimentally observed current can indeed be primarily attributed to the SWNT sidewall.

We can use the simulation routine as explained above to predict the diffusion-limited current for each specific device of Figure 2c. A linear regression of the simulated currents against the exposed lengths yields $i_{mt} = 36 \pm 1$ pA/μm. The experimental values of the mass-transport-limited current, extracted from the fits of the experimental curves, however, yielded $i_{mt} = 24 \pm 2$ pA/μm, which is 33% less than the simulated mass-transport-limited current. This difference may be attributed to several factors: First, the absence of supporting electrolyte causes a migrational contribution to the mass-transport-limited current. Using the method of Amatore et al.,[18] migration of $FcTMA^+$ will cause a 15% reduction of the mass-transport-limited current. Second, a partial blocking of the electroactive surface would also decrease the mass-transport-limited current.

The estimation of i_{mt} allows us to calculate the relevance of heterogeneous electrode kinetics. For a 1 μm long SWNT with a 1 nm radius in a $1 \times 1.5 \times 0.5$ μm ($L \times W \times H$) pit exposed to a $FcTMA^+$ solution with $k^0 \sim 4$ cm/s, we find that $K_0 \sim 0.4$, indicating that heterogeneous electrode kinetics should significantly affect the voltammetric wave shape. For comparison, the dimensionless rate constant of a hemispherical electrode is given by $K_0 = k^0 r/D$.[16] A dimensionless rate constant of 0.4 thus would require a 7.5 nm radius hemispherical electrode. However, the diffusion-limited current obtained from a 7.5 nm radius hemispherical electrode is merely $i_{mt} = 4.1$ pA, which is an order of magnitude smaller than the current calculated for the 1 μm long SWNT electrode. Therefore, the SWNT electrode allows electron transfer rates to be resolved at a higher current level and thus an accordingly better signal-to-noise ratio. This is a direct consequence of the very high surface area of a SWNT combined with its nanometer-sized critical dimension, its radius. In addition to the easy fabrication due to their micrometer-long lengths, a SWNT electrode therefore has significant advantages over other available nanoelectrodes. Figure 4d shows the deviation from nernstian behavior of the voltammetric wave shape at a SWNT electrode caused by Butler−Volmer kinetics, using $\alpha = 0.65$ and $k^0 = 4$ cm/s.

Our data show essentially the same electrochemical behavior for metallic and semiconducting SWNTs. To clarify how the electronic structure of SWNTs affects the electrochemical reaction rate, we employ a model that considers the structure of the electronic states on the electrode and on the reactants in solution. Careful consideration of the relevant capacitances is required: Because of the low density of electronic states (DOS) on a SWNT as compared to a typical metal, the liquid acts as a highly effective gate that easily changes the SWNT Fermi level. Figure 5a depicts the solution−SWNT interface, represented by the intrinsic SWNT quantum capacitance C_q in series with the capacitance of the electrical double-layer C_{dl}, which is formed by ions in solution attracted by the charge on the SWNT.[12,19] Varying

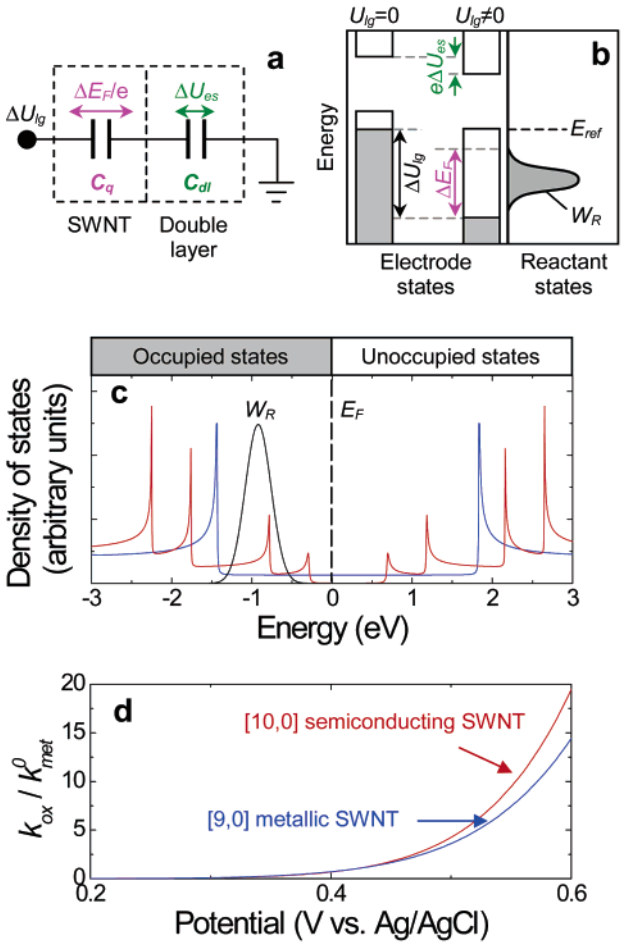

Figure 5. Effect of the electronic density of states on electrochemistry. (a) Schematic of the quantum capacitance and double-layer capacitance at the SWNT−liquid interface. (b) Energy diagram of the electrode and reactant states. The situation is drawn for a semiconducting electrode, though it is similarly applicable to a metallic electrode. $E = 0$ is defined as the potential of the reference electrode E_{ref}. Shaded regions indicate occupied electronic states. The electrode states are depicted for $U_{lg} = 0$ (where Fermi energy E_F and E_{ref} align) and $U_{lg} \neq 0$. The potential change ΔU_{lg} over the interface causes a chemical (ΔE_F/e) and electrostatic potential change (ΔU_{es}), where $\Delta U_{lg} = \Delta E_F/e + \Delta U_{es}$. (c) The overlap in energy of the occupied reactant states with the unoccupied SWNT states determines the rate of reaction. The SWNT states are depicted by the DOS of a metallic [9,0] SWNT (blue) and a semiconducting [10,0] SWNT (red). (d) Calculated k_{ox}/k^0_{met} as a function of U_{lg}, where k^0_{met} is the calculated oxidation rate for the metallic SWNT at $U = U^{0\prime}$. Calculations were done for $U^{0\prime} = 0.42$ V using a rough lower bound estimate of $\lambda = 0.5$ eV and the center of the SWNT band structures located at 0.2 eV (p-doping).

the applied potential U_{lg} over this interface results in changes both in the internal chemical potential of the SWNT, E_F/e, and the electrostatic potential U_{es} over the electrical double-layer such that $\Delta U_{lg} = \Delta E_F/e + \Delta U_{es}$, where $\Delta E_F/e = \Delta U_{lg} C_{dl}/(C_{dl} + C_q)$ and $\Delta U_{es} = \Delta U_{lg} C_q/(C_{dl} + C_q)$. Because of the low DOS of a SWNT, $C_q < C_{dl}$ by an order of magnitude and thus $\Delta U_{lg} \approx \Delta E_F/e$. A direct consequence of this ratio of the capacitances is that the charge on the SWNT and in the electrical double-layer changes very little during voltammetry in contrast with typical metallic electrodes. The applied potential largely tunes the SWNT Fermi energy instead of the potential over the double-layer. We estimate the rate of oxidation k_{ox} as depicted in Figure 5b and 5c, based on the integration over the occupied states of the reactants in solution that coincide in energy with the unoccupied states of the SWNT according to[20,21]

$$k_{ox}(U_{lg}) \propto \int_{-\infty}^{\infty} W_R(\lambda,E)[1 - f(E,U_{lg})]\rho(E,U_{lg})\, dE \quad (2)$$

Here the function $W_R(\lambda,E)$ represents the reactant states as a Gaussian distribution in the Gerischer−Marcus representation[20] as a function of the reorganization energy λ and energy difference E between SWNT and the plane of electron transfer. The functions $f(E,U_{lg})$ and $\rho(E,U_{lg})$ are respectively the Fermi−Dirac distribution and the SWNT DOS, both dependent on the applied potential U_{lg}. As a result of the small C_q, the SWNT DOS remains essentially fixed to the solution states.

It is known that the band-gap region of a semiconducting electrode can have a large effect on the observed electrochemical reaction rate. Despite the presence of a band gap in the semiconducting SWNT DOS, we observe that one obtains highly similar electrochemical responses from metallic and semiconducting SWNTs. This can be understood from the following points. From previous studies of similar water-gated SWNT devices it was found that the SWNTs are considerably p-doped.[12,19] Therefore, over the electroactive potential range of $FcTMA^+$, the Fermi level is likely below the band-gap region. A voltammetric sweep toward 0.6 V vs Ag/AgCl will lower the SWNT Fermi level even further away from the gap, increasing the amount of unoccupied states that promote the rate of oxidation of $FcTMA^+$. Second, electronic states away from the Fermi level contribute significantly to the rate of reaction due to the width of the reactant distribution, typically in the order of 1 eV, causing an averaging effect on the SWNT DOS. Figure 5d shows the calculated oxidation-rates for a [9,0] metallic and a [10,0] semiconducting SWNT. The result demonstrates that it is possible to obtain similar electrochemical behavior from metallic and semiconducting SWNTs. Extensive calculations of oxidation rates for SWNTs with different chiralities and diameters between 0.7 and 3 nm show that the apparent k^0 can vary by about a factor of 3.[21] This variation, however, is not directly correlated to the metallic or semiconducting nature of the SWNT, nor does it directly reflect the diameter of the SWNT. This variation is caused by the position of the van Hove singularities with respect to the energy of the reactant state. To what extent the experimentally observed variation of the apparent k^0 as presented in this report can be attributed to band-structure effects is not clear. Currently we are conducting experiments to address this issue in more detail.

In conclusion, we have presented the first demonstration of individual SWNTs as nanoelectrodes for electrochemistry. SWNTs appear to provide unique tools for both fundamental and applied electrochemical studies. We obtain a steady-state electrochemical current and a very high rate of electron transfer to the SWNT sidewall. Because of the nanometer diameter, the kinetics of fast electrode reactions can be

resolved. Therefore, an individual SWNT provides a straightforward and reproducible way to fabricate nanoelectrodes with a well-defined geometry capable of probing fast electrode kinetics at relatively high steady-state current levels. The characteristic and well-defined SWNT DOS creates an excellent opportunity to study the effect of the distinct electronic structure of the electrode on the rate of electron transfer. The high aspect ratio of a SWNT can be further exploited to fabricate a nanometer-sized local electrochemical probe. In addition, the possibility of functionalization of the SWNT nanoelectrode opens the route toward electrochemical single redox molecule studies.

Acknowledgment. We thank Bernadette Quinn for helpful discussions. This work was supported by the Netherlands Organization for Scientific Research (NWO) and the Foundation for Fundamental Research on Matter (FOM).

References

(1) Shao, Y. H.; Mirkin, M. V.; Fish, G.; Kokotov, S.; Palanker, D.; Lewis, A. *Anal. Chem.* **1997**, *69*, 1627.
(2) Slevin, C. J.; Gray, N. J.; Macpherson, J. V.; Webb, M. A.; Unwin, P. R. *Electrochem. Comm.* **1999**, *1*, 282.
(3) Katemann, B. K.; Schuhmann, W. *Electroanalysis* **2002**, *14*, 22.
(4) Chen, S.; Kucernak, A. *Electrochem. Commun.* **2002**, *4*, 80.
(5) Lemay, S. G.; Broek van den, D. M.; Storm, A. J.; Krapf, D.; Smeets, R. M. M.; Heering, H. A.; Dekker, C., submitted.
(6) Watkins, J. J.; Chen, J.; White, H. S.; Abruna, H. D.; Maisonhaute, E.; Amatore, C. *Anal. Chem.* **2003**, *75*, 3962.
(7) Dekker, C. *Phys. Today* **1999**, *52*, 22.
(8) Katz, E.; Willner, I. *ChemPhysChem* **2004**, *5*, 1084.
(9) Kong, J.; Soh, H. T.; Cassell, A. M.; Quate, C. F.; Dai, H. J. *Nature* **1998**, *395*, 878.
(10) Lin, Y.; Taylor, S.; Li, H.; Fernando, K. A. S.; Qu, L.; Wang, W.; Gu, L.; Zhou, B.; Sun, Y.-P. *J. Mater. Chem.* **2004**, *14*, 527.
(11) Williams, K. A.; Veenhuizen, P. T. M.; de la Torre, B. G.; Eritja, R.; Dekker, C. *Nature* **2002**, *420*, 761.
(12) Besteman, K.; Lee, J.-O.; Wiertz, F. G. M.; Heering, H. A.; Dekker, C. *Nano Lett.* **2003**, *3*, 727.
(13) Campbell, J. K.; Sun, L.; Crooks, R. M. *J. Am. Chem. Soc.* **1999**, *121*, 3779.
(14) The SiO_x layer avoids direct contact of the SWNTs with resist. Samples fabricated without this protective SiO_x layer were found to have significant contamination of the SWNT surface after lithography and displayed poor electrochemical performance. Although the contamination is reduced with the SiO_x layer, it was not entirely prevented.
(15) Tans, S. J.; Verschueren, A. R. M.; Dekker, C. *Nature* **1998**, *393*, 49.
(16) Zoski, C. G. In *Modern Techniques in Electroanalysis*; Vanysek, P., Ed.; Wiley: New York, 1996.
(17) Conyers, J. L.; White, H. S. *Anal. Chem.* **2000**, *72*, 4441.
(18) Amatore, C.; Fosset, B.; Bartelt, J.; Deakin, M. R.; Wightman, R. M. *J. Electroanal. Chem.* **1988**, *256*, 255.
(19) Rosenblatt, S.; Yaish, Y.; Park, J.; Gore, J.; Sazonova, V.; McEuen, P. L. *Nano Lett.* **2002**, *2*, 869.
(20) Bard, A. J.; Faulkner, L. R. *Electrochemical Methods, Fundamentals and Applications*, 2nd ed.; John Wiley & Sons: New York, 2001.
(21) Heller, I. et al. in preparation.

NL048200M